Performance of Two-Layer Reservoir Computing with van der Pol Oscillators

Yasufumi Kajino, Kazuki Yasufuku, Yoko Uwate, Yoshifumi Nishio
Dept. Electrical and Electronic Eng, Tokushima University
2-1 Minami-Josanjima, Tokushima 770-8506, Japan
Email: {kajino, yasufuku, uwate, nishio}@ee.tokushima-u.ac.jp

***Abstract*—We studied network reservoir computing using interconnected oscillators. One VDP (van der Pol) oscillator was considered as one node, and it was interconnected to form a reservoir layer. In this study, two-layer reservoir was used and its performance was evaluated. The input waveform generation task was compared between a single-layer (100 nodes) and a two-layer (50 nodes in each layer) reservoir. The results showed that the two-layer reservoir generated input waveform more faithfully than the single-layer reservoir when the input waveform were sine, triangle, and square waves. The accuracy was better with two-layer, but it depends on the input waveform.**

I. Introduction

Deep learning is a machine learning method based on artificial neural networks and has excellent performance in image, speech recognition, and natural language processing[1]-[5]. However, training large models requires a lot of computational time and resources, and it is also difficult to predict the time required for training. Since real-time time-series pattern recognition requires fast learning, machine learning models with low computational complexity and high performance are important.

Reservoir computing has attracted attention as a method with high accuracy while reducing energy and computational complexity compared to conventional AI models. Unlike traditional neural networks, reservoir computing mainly only requires operations at the readout layer and has its own dynamics of nonlinear projection of input into a high-dimensional space. This simplifies learning while still providing effective performance. Furthermore, reservoir computing has been implemented using a variety of physical systems, and its potential has been widely explored [6]-[8]. However, there are still gaps in our understanding of optimal architecture and performance maximization, and future research should focus on innovative reservoir design, enhanced learning algorithms, and integration with other AI techniques.

This research focuses on network reservoir computing using oscillators as computational elements. The coupled oscillator model is the basis for modeling and analyzing rhythmic behavior in ecology and neuroscience as well as engineering [9]-[12]. In particular, the synchronization phenomena of van der Pol oscillators, a simple yet versatile coupled system of nonlinear oscillators, has attracted a great deal of attention, which has helped to approximate various natural phenomena [13], [14].

Our research will improve the efficiency and accuracy of reservoir computing systems by increasing the number of reservoir layers to two, paving the way for a revolution in AI applications. We focus on exploring different configurations to develop energy-efficient, high-performance systems suitable for resource-limited environments.

II. Two-Layer Reservoir with Oscillator Circuit

In this study, two-layer reservoir using interconnected oscillators network is presented. Proposed reservoir computing is used the unique dynamics of oscillators. Fig. 1 shows an overview of the structure of two layers networked reservoir computing system.

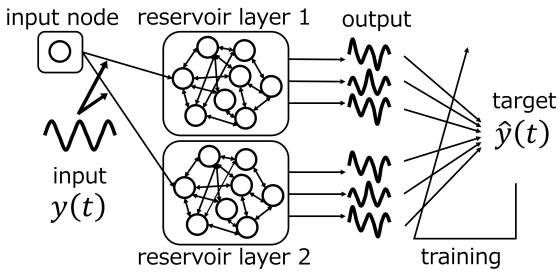

Fig. 1. Composition of the proposed two-layer reservoir

The input signal is input by adjusting the coupling strength between the input node and the reservoir layer. It is then input into the oscillator network as shown Fig. 1 and propagated by mutual coupling between oscillators. As a result, output signal is obtained from a number of output terminals located in the network. The output signal is obtained by measuring the voltage difference between each oscillator and the reference oscillator. It is important to note that the coupling strength in the reservoir layers is fixed throughout the calculation. In the readout layer, liner regression is performed. To evaluate the effectiveness of the proposed two-layer reservoir, we compared it with a single-layer reservoir.

van der Pol oscillators were used in this study. Fig. 2 shows its circuit model. van der Pol oscillator is a circuit consisting of a capacitance C, and inductance L, and a nonlinear resistor G connected in parallel.

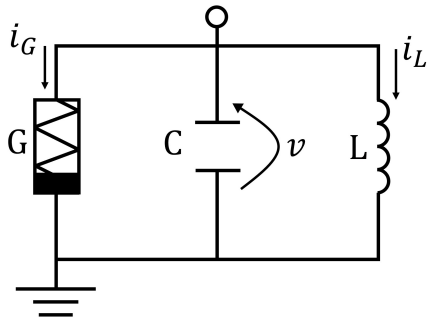

Fig. 2. Circuit model of van der Pol oscillator

In this experiment, the oscillators are connected with a resistor. The circuit equation of the VDP oscillator is expressed as follows:

$$\begin{cases} C\dfrac{dv_n}{dt} = -i_L - i_G - \displaystyle\sum_{n,k=1}^{N} \dfrac{1}{R_{nk}}(v_k - v_n) \\ L\dfrac{di_n}{dt} = v_n. \end{cases} \tag{1}$$

In this experiment, nonlinear resistors exhibiting third-order characteristics were used. The current-voltage characteristic of the nonlinear resistor is expressed as follows:

$$i_g = -g_1 v + g_3 v^3. \tag{2}$$

where $g_1, g_3 > 0$.

The circuit equation is normalized as follows using the normalization parameters. The normalization parameters and the normalization equations are shown in Eqs. (3) and (4).

$$\begin{cases} v = \sqrt{\dfrac{g_1}{g_3}}x, \;\; i = \sqrt{\dfrac{g_1 C}{g_3 L}}y, \;\; t = \sqrt{LC}\tau \\ \varepsilon = g_1\sqrt{\dfrac{L}{C}}, \;\; \gamma = \dfrac{1}{R}\sqrt{\dfrac{L}{C}} \end{cases} \tag{3}$$

$$\begin{cases} \dfrac{dx_n}{d\tau} = \varepsilon x_n(1 - x_n^2) - y_n - \displaystyle\sum_{n,k=1}^{N} K_{nk}(x_k - x_n) \\ \dfrac{dy_n}{d\tau} = x_n \end{cases} \tag{4}$$

N is the number of oscillators in each reservoir layer. K_{nk} is the coupling strength and represented by as follows:

$$K_{nk} = E_{nk}\gamma_{nk}. \tag{5}$$

Here, E_{nk} represents the adjacency matrix of the network. It indicates whether the kth oscillator is connected to the nth oscillator. If $E_{nk} = 1$, it means they are connected, $E_{nk} = 0$ indicates that they are not connected.

III. SIMULATION METHODS

For the input signal waveform, a data set of 60,000 sine, triangle, and square waves with amplitudes ranging from -1 to 1 was used. Each data point was input at 1τ intervals according to the Runge-Kutta method. The first 28,000 data sets were used for training and 32,000 for test. The Runge-Kutta method was used to simulate the oscillators by solving the normalized equations of the van der Pol oscillator. A moving average of the oscillators in the reservoir layer was taken, which was used as the output of the reservoir layer. Ridge regression was performed on the output waveform of the reservoir layer using the target waveform to find the optimal output weights. Ridge regression can be used to determine the output weights to achieve the desired performance.

Ridge regression is represented by the following equation where $\hat{W}_{out}$ is the output weight and D is the matrix of the teacher signal.

$$\hat{W}_{out} = DX^T(XX^T + \beta I)^{-1} \tag{6}$$

To evaluate the proposed model, the error between the output waveform using the optimal output weights and target waveform was measured. Since the simulation using the Runge-Kutta method showed a transient response in the initial $10{,}000\tau$, the error evaluation evaluation was performed on the results after $10{,}000\tau$. Normalized root mean square error (NRMSE) was used for error evaluation. In general, the root mean square error (RMSE) is used for error evaluation. However, RMSE is susceptible to outliers in data or predicts because it calculates the time-averaged square error of the squared error between the model output and the target output. NRMSE prevents this effect. NRMSE normalizes RMSE by the variance of the target output. RMSE and NRMSE are shown in Eqs. (7) and (8), where $y(n)$ is the input waveform and $d(n)$ is the target time series data.

$$RMSE = \sqrt{\frac{1}{T}\sum_{n=1}^{T} ||d(n) - \hat{y}(n)||} \tag{7}$$

$$NRMSE = \frac{RMSE}{\dfrac{1}{T}\displaystyle\sum_{n=1}^{T} ||d(n) - \hat{d}(n)||} \tag{8}$$

The values of each parameter are as follows. Coupling probability p is $p = 0.8$. Coupling strength s is $s = 0.05$. Number of oscillators in two-layer reservoir N_1 and N_2 are $N_1 = N_2 = 50$. Number of oscillators in reservoir layer when single-layer N is $N = 100$.

The simulation was performed with different parameters for each layer. However, the best accuracy was obtained when the parameters were the same for both layers. Therefore, the simulation results are shown for the same parameters for both layers.

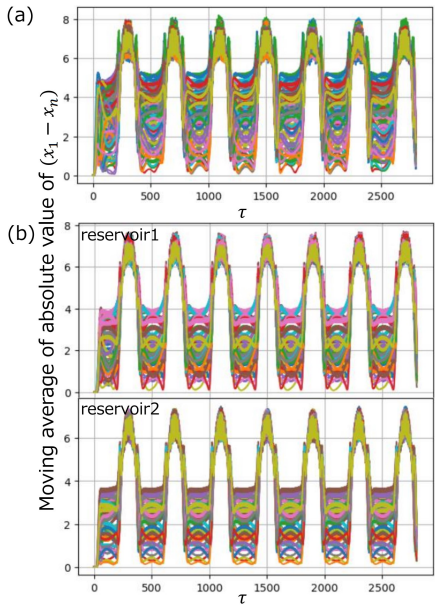

Fig. 3. Output during training of reservoir with sine wave input. (a) single-layer reservoir. (b) two-layer reservoir.

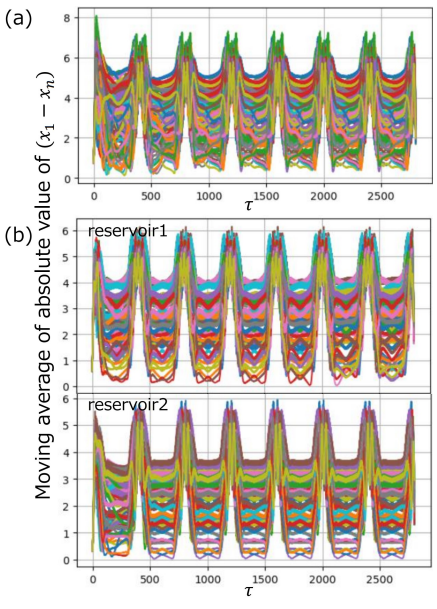

Fig. 4. Output during training of reservoir with triangle wave input. (a) single-layer reservoir. (b) two-layer reservoir.

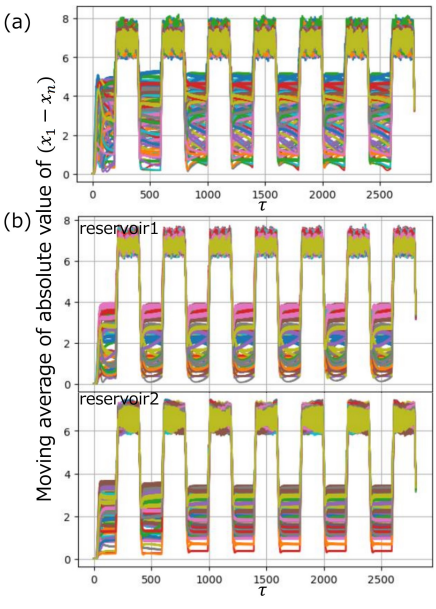

Fig. 5. Output during training of reservoir with square wave input. (a) single-layer reservoir. (b) two-layer reservoir.

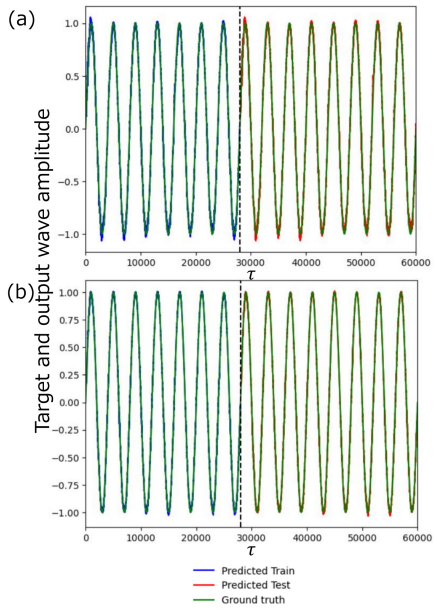

Fig. 6. Results of the waveform generation task. (a) single-layer reservoir. (b) two-layer reservoir. Input waveform is sine wave.

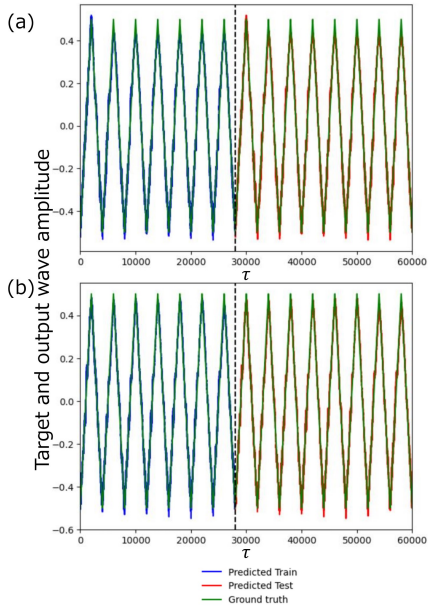

Fig. 7. Results of the waveform generation task. (a) single-layer reservoir. (b) two-layer reservoir. Input waveform is triangle wave.

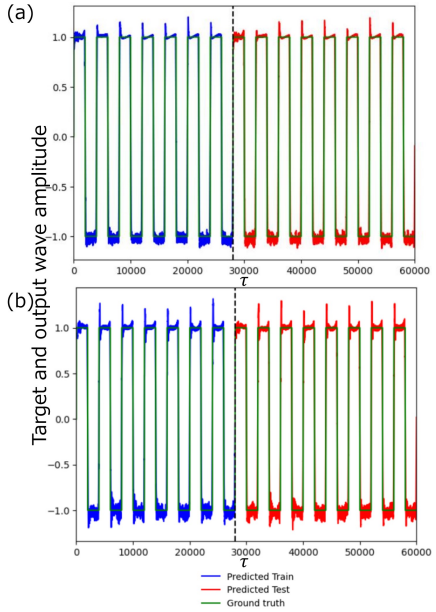

Fig. 8. Results of the waveform generation task. (a) single-layer reservoir. (b) two-layer reservoir. Input waveform is square wave.

TABLE I
ERROR EVALUATION OF INPUT WAVEFORM GENERATION TASK WITH SINGLE-LAYER AND TWO-LAYER RESERVOIR (NRMSE)

input waveform	sine wave		triangle wave		square wave	
	single-layer	two-layer	single-layer	two-layer	single-layer	two-layer
train	0.0443	0.0281	0.0938	0.0844	0.1741	0.1664
test	0.0491	0.0288	0.0935	0.0857	0.1764	0.1686

IV. SIMULATION RESULTS

This section presents the results of the simulations conducted. The output waveform of the reservoir when the input waveform is a sine wave is shown in Fig. 4. The output waveform of the reservoir when the input waveform is a triangle wave is shown in Fig. 5. The output waveform of the reservoir when the input waveform is a square wave is shown in Fig. 6. As parameter values ε is $\varepsilon = 0.1$. The results of the input waveform generation task are also shown in Figs. 7, 8, and 9. The green line represents the target waveform, the blue line represents the training output, the red line represents the test output. The training and verification errors are summarized in Table I.

The graphs in Figs. 4, 5, and 6 show that a two-layer reservoir with 50 nodes in each layer has a response closer to the input waveform than a single-layer reservoir with 100 nodes. Referring to Table I, when comparing the single-layer and two-layer when the input wave is sine wave, the two-layer has a learning error of 0.0162 and a test error of 0.0203 smaller. when the input wave was a triangle wave, comparing a single-layer to a two-layer, the training error was 0.0094 and the test error was 0.0078 smaller with two-layer. Furthermore, when the input wave was a square wave, comparing a single-layer to a two-layer, the training error was 0.0077 and the test error was 0.0078 smaller with two-layer. As can be seen from Fig. 8, the output waveform does not reproduce the input waveform well when the amplitude takes a constant value with respect to the passage of time.

V. CONCLUSIONS

We have increased the number of network reservoir layers with interconnected oscillators and investigated their performance. The proposed reservoir computing approach is superior to other types of reservoirs in terms of flexible reservoir layer design. Specifically, we focused on the VDP oscillator and performed the task of input waveform generation. The accuracy of the input waveform generation task was particularly improved when the input waveform was a sine wave, while Other waveforms did not show much improvement in accuracy compared to the sine wave. However, for all three waveforms, the two-layer reservoir was more faithful to the input waveform than the single-layer reservoir. These results highlight the importance of carefully selecting and setting the total number of reservoir layers and nodes. Flexibility in the choice of materials comprising the reservoir and in structural design offers the potential for further advances in this area.

In this study, it was not possible to clarify the role of each layer with respect to the input signal because the accuracy was improved when both layers had the same parameters. As a future prospect, we would like to evaluate the output and accuracy of each reservoir layer by switching the input signal in time and inputting it to reservoir layer 1 and reservoir layer 2.

REFERENCES

[1] Y. LeCun, Y. Bengio, and G. Hinton, "Deep learning, "Nature, vol.521, pp.436-444, 2015.

[2] Jacob Devlin, Ming-Wei Chang, Kenton Lee, Kristina Toutanova, "BEAT: Pre-training of Deep Bidirectional Transformers for Language Understanding"

[3] Li, Jinyu. "Recent advances in end-to-end automatic speech recognition." APSIPA Transactions on Signal and Information Processing 11.1, 2022.

[4] Wu, Zifeng, Chunhua Shen, and Anton Van Den Hengel. "Wider or deeper: Revisiting the resnet model for visual recognition." Pattern Recognition 90 pp.119-133, 2019.

[5] Chowdhary, KR1442, and K. R. Chowdhary. "Natural language processing." Fundamentals of artificial intelligence pp.603-649, 2020.

[6] Yuki Usami et al. "In-Materio Reservoir Computing in a Sulfonated Polyaniline Network." Adv.Mater,33,210268,2021.

[7] Sang-Gyu Koh et al."Reservoir computing with dielectric relaxation at an electrode-ionic liquid interface." Scientific Reports, 12:6958, 2022.

[8] Taro Kanao et al. "Reservoir Computing on Spin-Torque Oscillator." arXiv:1905.07937v2, 2019.

[9] Bonilla, L. L., Pérez Vicente, C. J., & Spigler, R, Time-periodic phases in populations of nonlinearly coupled oscillators with bimodal frequency distributions. Physica D: Nonlinear Phenomena, 113(1), 79-97, 1998.

[10] Hoppensteadt, F. C., & Izhikevich, E. M, Weakly Connected Neural Networks (Vol. 126). Springer Science & Business Media, 2012.

[11] Debbouche, N., Ouannas, A., Momani, S., et al, Fractional-order biological system: chaos, multistability and coexisting attractors. The European Physical Journal Special Topics, 231, 1061-1070, 2022.

[12] Ahn, S., & Rubchinsky, L. L, Temporal patterns of dispersal-induced synchronization in population dynamics. Journal of Theoretical Biology, 490, 110159, 2020.

[13] Weaam Alhejaili, Alvaro H. salas, S.A. El-Tantawy. "Approximate solution to a generalized Van der Pol equation arising in plasma oscillations." AIP Advances 12, 105104, 2022.

[14] Ayaz Hussain Bukhari et al, "Design of intelligent hybrid NAR-GRNN paradigm for fractional order VDP chaotic system in cardiac pacemaker with relaxation oscillator." Chaos, Solitons & Fractals vol.175, Part2, 114047, 2023.